Journal of Applied Polymer Science

Compatibilization of poly(lactic acid)/ethylene-propylene-diene rubber blends by using organic montmorillonite as a compatibilizer

Sisi Wang,[1] Sujuan Pang,[1] Lisha Pan,[1] Nai Xu,[1] Hanxiong Huang,[2] Tan Li[3]

[1]College of Materials and Chemical Engineering, Hainan University, Hainan, Haikou 570228, People's Republic of China
[2]Lab for Micro Molding and Polymer Rheology, Department of Industrial Equipment and Control Engineering, South China University of Technology, Guangzhou 510640, People's Republic of China
[3]Shiner Industrial Co, Ltd, Hainan, Haikou 570125, People's Republic of China
Correspondence to: Nai Xu (E-mail: xunai@hainu.edu.cn) or Hanxiong Huang (E-mail: mmhuang@scut.edu.cn)

ABSTRACT: This work focuses on phase morphology and properties of immiscible poly(lactic acid)/ethylene-propylene-diene rubber (PLA/EPDM) blends compatibilized with organic montmorillonite (OMMT). Effect of OMMT loading on phase morphology, mechanical properties, and blown film bubble stability was investigated. Transmission electron micrographs show that a large number of OMMT nanolayers locate at interfacial region between PLA and EPDM phase, as well as in EPDM phase due to higher affinity of OMMT with EPDM. Scanning electron micrographs show that EPDM domain size decreases largely with increasing OMMT loading, which is associated with reduction of interfacial energy and inhibition of coalescence by the OMMT locating at the interface, acting as an emulsifier to enwrap the discrete domains. As OMMT loading increases from 0 to 1 phr, elongation at break increases from 20.4 to 151.7% and notched impact strength is enhanced from 8.2 to 31.7 $kJ \cdot m^{-2}$. The reduced EPDM domain is the main reason for enhanced toughness of PLA/EPDM/OMMT samples according to crazing with shear yielding mechanism. However, with more than 2 phr of OMMT, the toughness decreases largely due to excessive stress concentration and OMMT aggregation. Attempts were made to produce ductile films from the PLA/EPDM/OMMT nanocomposites by using blown film extrusion. Improvement in blown film bubble stability and tensile ductility of PLA/EPDM/OMMT films also shows that OMMT is an efficient compatibilizer, as well as a processing aid for PLA/EPDM blends. © 2016 Wiley Periodicals, Inc. J. Appl. Polym. Sci. **2016**, *133*, 44192.

KEYWORDS: biopolymers & renewable polymers; clay; compatibilization; elastomers; films

Received 31 January 2016; accepted 17 July 2016
DOI: 10.1002/app.44192

INTRODUCTION

Bio-based poly(lactic acid) (PLA) is a novel kind of linear aliphatic thermoplastics, which is produced from renewable resources, such as corn and wheat straw. PLA is an attractive candidate for replacing petrochemical polymers due to its biocompatibility and renewability. PLA has reasonably good mechanical, optical, and barrier properties compared to general petroleum-based polymers. The growing demands of PLA can be expected for many applications, such as household field, industry, biomedical items.[1]

However, inherent brittleness of PLA greatly limits its applications. Blending with elastomers or flexible resins, such as polyurethane, polyamide elastomer, polyethylene, poly(caprolactone), poly(butylene succinate), and poly(butylene adipate-*co*-terephthalate), is an effective and economical method to improve the ductility of PLA.[2–8]

Ethylene-propylene-diene rubber (EPDM) is the copolymer of ethylene, propylene, and a small number of conjugated dienes. As an elastomer, EPDM has been widely used to toughen brittle polymers, such as polypropylene[9] and nylon.[10] In view of its good performance, EPDM is considered as a good candidate for the toughening of PLA. However, the distinct incompatibility between hydrophobic EPDM and hydrophilic PLA usually weakens the toughening effect of EPDM on PLA matrix. Hence, compatibilization between PLA and EPDM has to be increased to improve the mechanical performance of PLA/EPDM blends.

In the past 15 years, some reports have proposed that a number of rigid nanoparticles (e.g., PP/PS/nano-SiO_2,[11] PP/EPDM/nano-SiO_2,[12] PS/PMMA/OMMT,[13] PLA/EVA/MWCNTs,[14] PLA/TPU/nano-TiO_2,[15] PLA/TPU/nano-SiO_2[16]) can be used as compatibilizers to tailor the interface, making blends perform better. The decreased size of dispersed phases is attributed to reduction of interfacial energy and inhibition of coalescence by the presence of a solid barrier around the dispersed phase. Gelfer *et al.*[13] prepared PS/PMMA blends with organoclays by melt mixing method. They found that the majority of organoclay

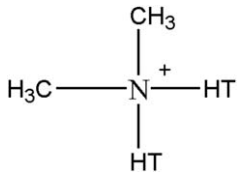

Figure 1. Chemical structure of dimethyl dihydrogenated tallow ammonium (HT: hydrogenated tallow).

particles concentrated in the PMMA phase and at the interfacial region between PS and PMMA. Due to the selective distribution of organoclay and its compatibilization effect on PS and PMMA phases, the microdomain size showed a drastic reduction. Shi *et al.*[14] investigated the effect of multiwalled carbon nanotubes (MWCNTs) on microstructure and mechanical properties of PLA/EVA blends. It was confirmed that MWCNTs had a tendency to migrate from PLA phase to EVA phase and mainly distributed at the interface. In addition, the nanocomposites exhibited enhanced ductility because the selective distribution of MWCNTs improved the interfacial properties of PLA/EVA blends. Xiu *et al.*[15] investigated the selective distribution of TiO_2 nanoparticles in PLA/TPU blends. It was interesting to find that, regardless of the method of TiO_2 introduction, the nanoparticles were always selectively localized at the phase interface between PLA and TPU, leading to a significant improvement in toughness.

Overall, the above researches provide a potential and simple method to improve the compatibility of immiscible PLA blending system. So far, few studies of compatibilizing PLA/EPDM blend have been reported in literature. In this work, organic montmorillonite (OMMT) was used as a physical compatibilizer to improve the compatibility of immiscible PLA/EPDM blend and refine the size of EPDM domains. The selective localization and compatibility mechanism of OMMT were discussed. And then, the effect of morphological change on ductility of PLA/EPDM/OMMT was characterized and discussed in detail. Furthermore, film-blowing processes for PLA/EPDM/OMMT nanocomposites were investigated preliminarily. The effect of OMMT on the blown film bubble stability and tensile ductility of the obtained films was investigated.

EXPERIMENTAL

Materials

Commercial PLA, trade name Natureworks 4032D, exhibits a density of 1.24 g·cm^{-3} and a melt flow index of 3.3 g·10 min^{-1} (190 °C, 2.16 kg). EPDM, trade name 3722P with a density of 0.86 g·cm^{-3}, was supplied by Dow. OMMT (trade name 1.44PSS) modified with dimethyl dihydrogenated tallow ammonium was purchased from Nanomer. Chemical structure of the modifier is shown in Figure 1.

Sample Preparation

A co-rotating twin screw extruder (SHJ-20, Giant Co. Ltd., China) equipped with a volumetric feeder and a strand pelletizer was employed to prepare PLA/EPDM/OMMT nanocomposites. The extruder screw had a diameter of 20 mm and an *L*/*D* ratio of 40. Before extrusion, the PLA and EPDM were dried in a vacuum oven at 50 °C for 10 h. OMMT was dried in an air oven at 110 °C for 5 h.

First, binary mixture of PLA/EPDM was prepared to achieve a best recipe of binary blend. PLA/EPDM was denoted as *X*/*Y* by mass fraction (binary mixtures of the mass ratios of 100/0, 95/5, 90/10, 85/15, 80/20, and 70/30 were prepared). PLA and EPDM were premixed and then fed into the twin-screw extruder. The temperatures were independently controlled at six zones along the extruder barrel and a strand die to achieve a temperature profile ranging from 150 to 185 °C.

In accordance with the above method, PLA/EPDM/OMMT (90/10/x) nanocomposites with various OMMT loadings were also prepared. Here, the resulted nanocomposites are referred as PLA/EPDM/OMMT (90/10/*x*), where 90/10 denotes weight ratio of PLA/EPDM, and *x* denotes OMMT parts per hundreds of total resin (phr). In this work, *x* is 0, 0.5, 1, 2, 3, and 5 phr, respectively. To research the effect of OMMT on the mechanical property of PLA, PLA/OMMT (100/*x*) nanocomposites with various OMMT loadings were also prepared.

And then, the obtained extrudates were compression molded under 210 °C and 15 MPa within 8 min to achieve sheets. Standard dumbbell tensile specimens and notched impact specimens were prepared from the sheets using a universal sampling machine (WZY-240, Chengde Hengtong Test Instrument Co., Ltd, China).

Blown-Film Extrusion Process

Neat PLA, PLA/EPDM (90/10), as well as PLA/EPDM (90/10) with 1 and 2 phr OMMT samples were melt-compounded using the co-rotating twin screw extruder. The extrudates were pelletized. And then the pellets were fed into a single screw extruder (LSJ-20, Shanghai Kechuang Plastic Machinery Factory, China) with a 20-mm-diameter screw and a L/D of 25 to blow films. The temperatures at different zones were independently controlled in order to achieve a temperature profile in the range of 165–190 °C. An annular die with a diameter of 34 mm and die gap of 0.5 mm was used to shape the initial tube dimensions. The screw speed was set at 25 rpm and the taken up speed was set to 1.65 m·min^{-1}. When the blown-film extrusion process started up, pressure air was introduced at the bottom of the die to inflate the bubble. The size of the bubble was maintained at a certain internal pressure. And then, the blown tube was flattened in the nip rolls and taken up by the winder. Finally, a roll of film was obtained. In the experiment, the obtained films have a mean thickness ranged from 60 to 100 μm. Blown-up ratio (ratio of bubble diameter to die diameter, BUR) is ranged from 1.5 to 2.0, and taken-up ratio (ratio of film taken-up velocity to the melt velocity at the die exit, TUR) is around 5.5. These two parameters provide indications of the microstructure orientation as a result of stretching in length transversal to the taken-up direction (TD, for BUR,) and length parallel to the taken-up direction or machine direction (MD, for TUR). Similar method was taken to blow film in some literature. [17,18]

Mechanical Properties

Tensile testing was performed with a XLW universal tensile testing machine (Jinan Languang Mechanical and Electrical

Technology Co., Ltd, China) at a across-head speed of 25 mm·min^{-1}, according to standard GB/T1040-1992. The results obtained were averaged at least five specimens. Notched izod impact strength was measured according to standard GB/T 1843-2008 using an XJU-5.5 pendulum impact tester (Chengde Dahua Machine Co., Ltd, China). Pendulum impact velocity was 3.5 m·s^{-1} and the results were an average of ten specimens.

In addition, tensile properties of the blown films were tested with a crosshead speed of 50 mm·min^{-1}. Rectangular specimens with a width of 15 mm were cut from the blown film.

SEM Observation

Cryo-fractured surfaces and notched impact fracture surfaces of the specimens were examined using scanning electron microscope (SEM) (S-3500N Hitachi). All the specimens were sputter coated with gold prior to examination.

Particle size distribution of EPDM phase was analyzed by Nano Measure software. The mean particle size (d_{mean}), minimum and maximum particle size (d_{min} and d_{max}) can be shown by the software.

TEM Observation

Dispersions of OMMT in the blends were observed by a transmission electron microscope (TEM) (JEM-2010 Japan) with a 100-kV accelerating voltage. The transmission electron micrographs were taken from microtomed sections in thickness of 80–100 nm.

XRD Analysis

Swollen degree of OMMT was determined using a D8 advance X-ray diffractometer (XRD) (BRUKER AXS, Germany) using Cu-Kα X-ray source (λ = 1.542 Å) operated at 40 kV and 40 mA. Data were recorded in 2θ range of 2°–10° at the scan rate of 1°·min^{-1}.

RESULTS AND DISCUSSION

Mechanical Properties and Micromorphology of PLA/EPDM Binary Blends

Tensile properties and impact strength of PLA/EPDM binary blends with different mass ratios were measured, and the results are presented in Figure 2. It can be seen from Figure 2(A) that, with increasing EPDM content, elongation at break of PLA/EPDM blends increased first and then dropped. The elongation at break of neat PLA was only 3.5%, showing a classic brittle fracture behavior. When 10 wt % of EPDM was blended with PLA, the elongation at break only increased from 3.5% to the maximum value of 20.4%. With further increasing EPDM content, the elongation at break of samples showed an obvious decrease. Similar to the elongation at break, notched impact strength also showed a same dependence on EPDM content as shown in Figure 2(B). When the EPDM content increased from 0 to 10%, the impact strength increased from 4.8 kJ·m^{-2} to the maximum value of 8.2 kJ·m^{-2}. And then, the notched impact strength showed a small decrease with further increasing the EPDM content.

The results of tensile and impact performances suggest that EPDM shows a weak toughening effect on PLA matrix. The limited increment in toughness is attributed to low compatibility between PLA and EPDM, resulting in less interfacial adhesion. The less interfacial adhesion would lead to debonding of

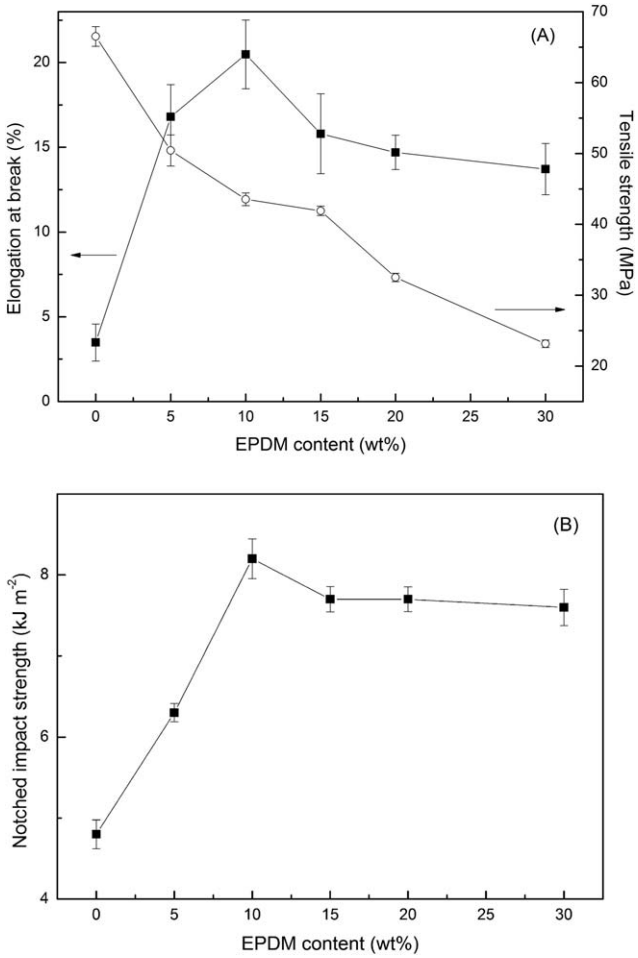

Figure 2. Curves of (A) tensile properties and (B) impact strength vs. EPDM content of PLA/EPDM blends.

EPDM particles from PLA matrix and induce premature cracks under stress.

In order to investigate the compatibility and micromorphology of PLA/EPDM blends with various EPDM contents, SEM observation was carried out. SEM micrographs and the corresponding average diameter (d_{mean}) of PLA/EPDM blends are shown in Figure 3, data of d_{mean} are tabulated in Table I. As shown in Figure 3(A) and Table I, the PLA/EPDM (90/10) blend showed a typical "sea island" structure. Moreover, the average size of EPDM domain was 2.5 μm and an obvious interface debonding phenomenon was observed at the interface between PLA matrix and EPDM particles. With further increasing the EPDM content, the EPDM domain size increased largely, and the debonding phenomena became more conspicuous, as shown in Figure 3(B,C). The main reason behind this is the incompatibility between the hydrophobic EPDM and hydrophilic PLA. As a result, the less interfacial adhesion and larger EPDM particles induced premature cracks and propagation under stress, leading to a sharp drop in material performance.

Micromorphology and Mechanical Properties of PLA/EPDM/OMMT (90/10/x) nanocomposites

In order to enhance the toughening effect of EPDM on PLA matrix, the organic modified OMMT was used as a

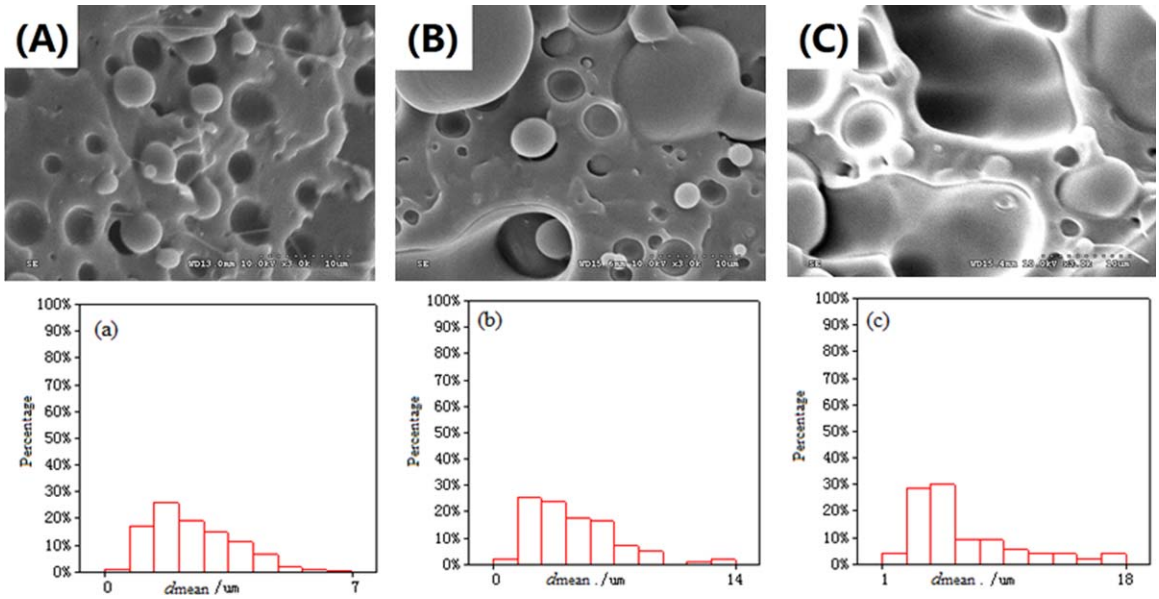

Figure 3. SEM micrographs of cryo-fractured surfaces and corresponding d_{mean} of PLA/EPDM blends: (A,a) 90/10; (B,b) 85/15; (C,c) 70/30. [Color figure can be viewed in the online issue, which is available at wileyonlinelibrary.com.]

compatibilizer to improve the interfacial property and reduce the EPDM domain size. The mass ratio of PLA/EPDM was fixed at the optimal ratio of 90:10 for the following study. The similar polarity of OMMT and EPDM might impel the OMMT nanoparticles to selectively distribute at the interface or in EPDM phase. Hence, the effect of OMMT loading on microstructure and mechanical properties of PLA/EPDM (90/10) was investigated in this section.

SEM micrographs and corresponding d_{mean} of PLA/EPDM/OMMT (90/10/x) with various OMMT loadings are shown in Figure 4 and Table I (corresponding d_{mean} of PLA/EPDM/OMMT (90/10/3) is not listed because of the blurry phase interface making it hard to calculate its d_{mean}). Obviously, these samples exhibited typical "sea-island" morphology, where discrete EPDM spherical domains uniformly dispersed in the PLA matrix. A size reduction of EPDM domains and a simultaneous improvement in size distribution can be seen with incorporation of OMMT compared with blank PLA/EPDM (90/10) blend without OMMT in Figure 3(A). SEM micrographs indeed show that the presence of OMMT obviously improves the compatibilization of immiscible PLA/EPDM blends. This result is similar to that usually seen in some polymer blends filled with other nanofillers, such as PP/EPDM/nano-SiO_2,[12] PP/EVA/CNT,[19] HDPE/NYLON6/CNT,[20] and PLA/LLDPE/OMMT,[5] where the size of dispersed-phase domains decreased significantly with adding small amount of nanofillers.

The size refinement of dispersed phase should be attributed to the selective localization of OMMT nanoparticles at the interface between PLA matrix and EPDM dispersed phase. TEM micrographs can provide further explanation of morphological information. TEM micrographs of PLA/EPDM/OMMT samples with 1–3 phr OMMT are presented in Figure 5. The typical two-phase structure can be seen in these TEM micrographs, in which the dark grey and white parts correspond to EPDM domains and PLA matrix, respectively. As can be seen from Figure 5, a large number of OMMT nanoparticles concentrated at interfacial region between PLA and EPDM phases, as well as in EPDM phase due to the fact that the OMMT nanoparticles modified by dimethyl dihydrogenated tallow ammonium had a higher affinity with EPDM domain. The similar result also was reported in PLA/LLDPE/OMMT nanocomposites.[5] Figure 6 schematically shows the OMMT selective localization at the interface of EPDM when EPDM and PLA were melt mixed. The decrease in EPDM domain size was resulted from reduction of interfacial energy and inhibition of coalescence by the presence of a solid barrier around the dispersed phase or localization of some OMMT nanoparticles at the interface, acting as the emulsifier to enwrap the discrete domains. This interfacial

Table I. Mean Particle Size of EPDM Dispersed Phase in the PLA/EPDM and PLA/EPDM/OMMT samples

Sample	$d_{min.}$ (μm)	$d_{max.}$ (μm)	d_{mean} (μm)	S_d (μm)
PLA/EPDM (90/10)	0.60	6.56	2.50	1.27
PLA/EPDM (85/15)	0.90	13.63	4.59	2.74
PLA/EPDM (70/30)	1.55	17.36	6.60	4.12
PLA/EPDM/OMMT (90/10/1)	0.71	2.26	1.36	0.55
PLA/EPDM/OMMT (90/10/2)	0.20	1.09	0.57	0.27

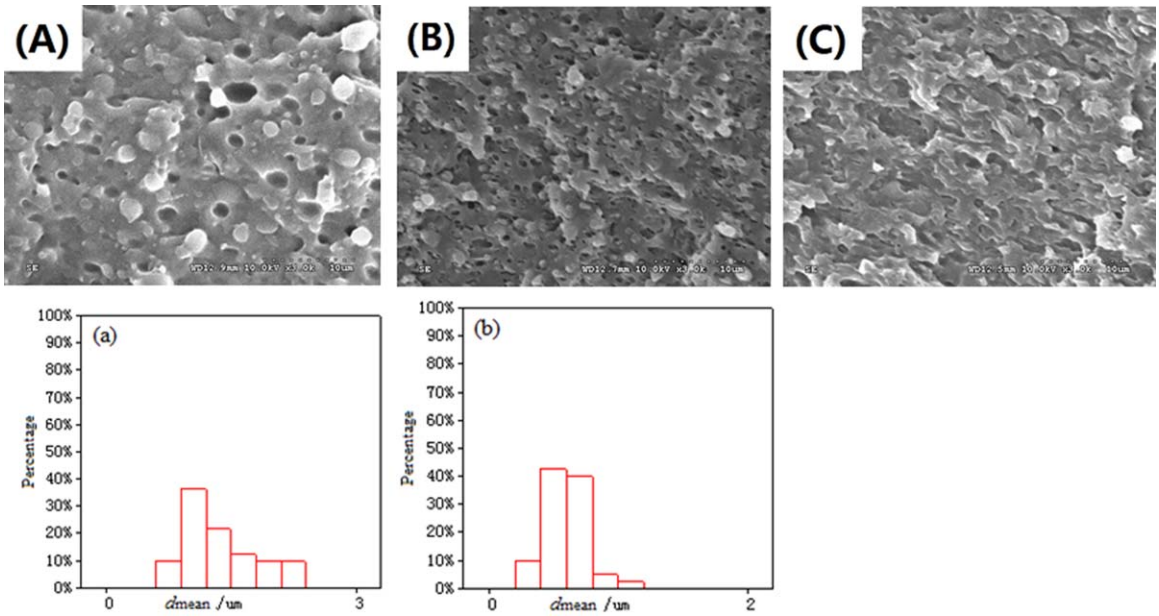

Figure 4. SEM micrographs of cryo-fractured surfaces and corresponding d_{mean} of PLA/EPDM/OMMT samples with various OMMT loadings: (A) PLA/EPDM/OMMT (90/10/1); (B) PLA/EPDM/OMMT (90/10/2); (C) PLA/EPDM/OMMT (90/10/3). [Color figure can be viewed in the online issue, which is available at wileyonlinelibrary.com.]

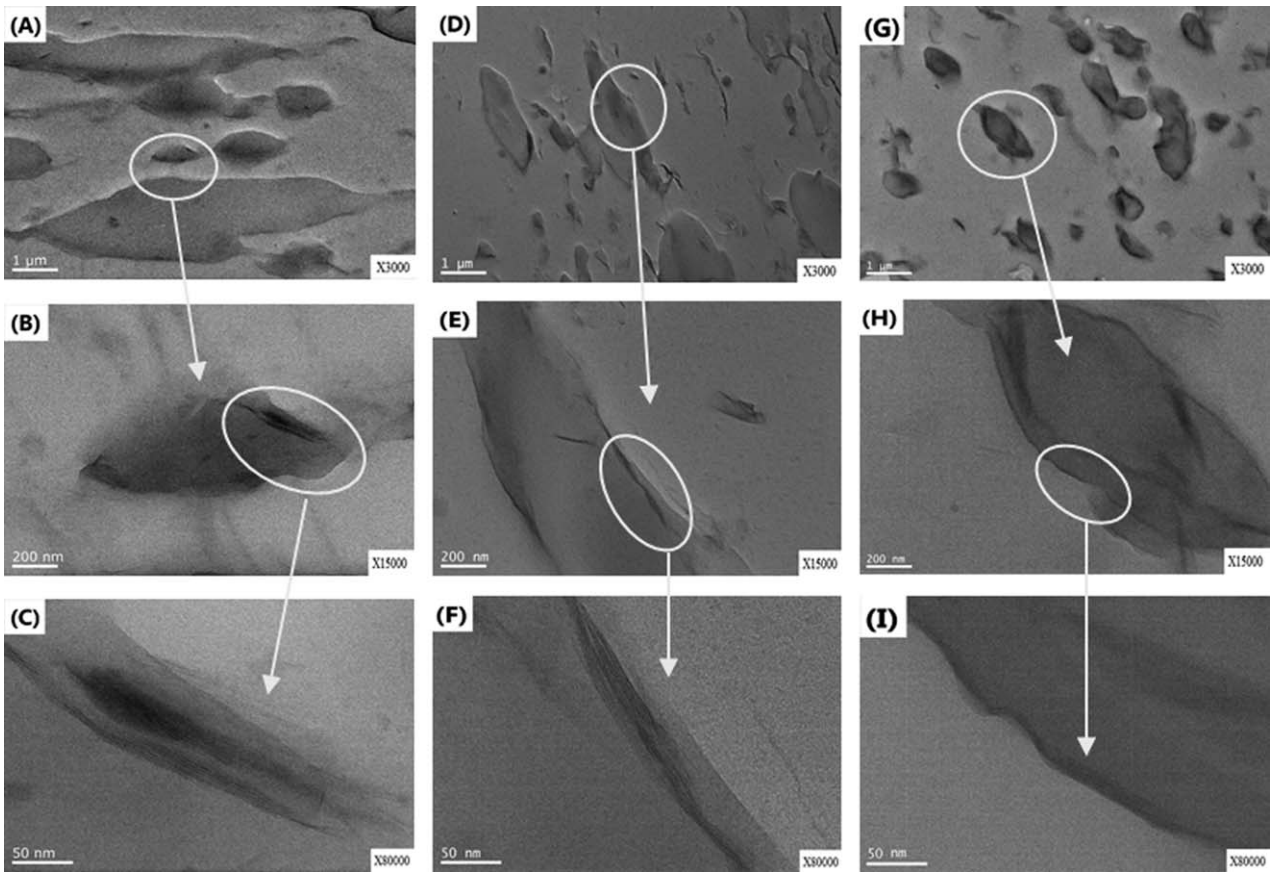

Figure 5. TEM micrographs for (A,B,C) PLA/EPDM/OMMT (90/10/1); (D,E,F) PLA/EPDM/OMMT (90/10/2) and (G,H,I) PLA/EPDM/OMMT (90/10/3) samples with various magnifications.

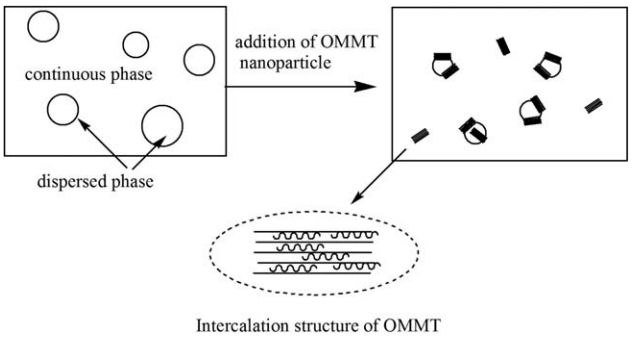

Figure 6. Schematics for selective localization of OMMT in PLA/EPDM blend.

localization of OMMT also can prevent the coalescence of EPDM domains effectively which helps compatibilization during melt mixing. Undoubtedly, OMMT nanoparticles showed a strong compatibilization effect on the immiscible PLA/EPDM system, leading to a refinement in size of EPDM phase.

Moreover, as shown in Figure 5(C,F,I), a distinctly intercalated microstructure of OMMT in the PLA/EPDM/OMMT samples was observed. To make clear the intercalating pattern of OMMT in these samples, XRD analysis was used. Orderly arranged montmorillonite silicate layers will show a corresponding diffraction peak in XRD patterns. The interlayer space of montmorillonite can be calculated according to the Bragg equation:

$$\sin\theta = n\lambda/2d$$

where, λ refers to the wavelength of diffraction ray Cu-Kα (λ = 1.542 Å), d stands for space between diffracting lattice planes and θ equals to diffraction peak value measured.

Figure 7 shows X-ray diffraction patterns of OMMT powders and the PLA/EPDM/OMMT (90/10/x) samples. As it is seen from Figure 7, pristine OMMT showed the (d_{001}) diffraction at $2\theta = 3.56°$, corresponding to an interlayer space of 2.48 nm. The characteristic (d_{001}) of OMMT in PLA/EPDM/OMMT (90/10/x) samples shifted to $2\theta = 2.5°$ approximately corresponding to a space of about 3.53 nm, which indicated that a few of macromolecular chains intercalated into the OMMT galleries, forming an intercalated structure at these PLA/EPDM/OMMT samples.

Figure 8 shows the elongation at break and tensile strength of PLA/EPDM/OMMT (90/10/x) samples with various OMMT loadings. It is found that the incorporation of OMMT gave rise to a significant improvement on the elongation at break of PLA/EPDM/OMMT (90/10/x). As OMMT loading increased to 1 from 0 phr, the elongation at break increased from 20.4% to the maximum value of 151.7%. And then, the elongation at break showed a decrease with further increasing OMMT loading. Furthermore, to investigate the effect of OMMT on the tensile ductility of PLA matrix, the tensile performance of PLA/OMMT (100/x) with various OMMT loadings also are presented in Figure 8. It can be pointed out that the incorporation of OMMT could improve the elongation at break of PLA slightly (from 3.5% for neat PLA to 4.3% with 1 phr OMMT) without EPDM, which is in accordance with the literature.[21] However, compared to the minor toughening effect of OMMT on PLA/OMMT samples, the incorporation of OMMT made a stronger enhancement in the ductility of these PLA/EPDM/OMMT samples due to the great compatibilizing effect of OMMT in the immiscible PLA/EPDM blends. In addition, the tensile strength of PLA/EPDM/OMMT fell gradually when the OMMT loading increased from 0 to 5 phr.

The inserted picture in Figure 8 presents photographs of tensile-fractured samples. The PLA/EPDM (90/10) samples showed a yielding with subsequent immediate failure under the tensile load. Compared with the blank PLA/EPDM (90/10) sample, PLA/EPDM/OMMT (90/10/0.5), PLA/EPDM/OMMT (90/10/1) and PLA/EPDM/OMMT (90/10/2) samples showed clear yielding behaviors upon stretching, and then the strain developed continuously. Finally, the samples broke at a significantly increased elongation.

It is obvious that the incorporation of OMMT in appropriate proportion can largely improve the ductility of PLA/EPDM (90/10) blend. The improvement in tensile ductility can be explained by elastomer toughening mechanism. According to the inserted picture in Figure 8, it is found that all PLA/EPDM/OMMT (90/10/x) samples showed a similar tensile yield behavior. In addition, necking and whitening phenomena can be found simultaneously when these samples were cold drawn under tensile test. According to the crazing with shear yielding mechanism, when EPDM content is constant, the size reduction of EPDM particles certainly leads to an increase in the number of EPDM particles in PLA matrix, as shown in Figures 3(A) and 4(A,B), that is helpful to terminate a craze extension and prevent a microscopic crack initiation and propagation, allowing for a considerable plastic deformation to develop.[22] However, when OMMT loading increases to 3 phr, the average size of EPDM domains decrease to less than 1 μm, which is hard to measure due to the fuzzy phase interface, as shown in Figure 4(C). Generally, when the dispersed phase size becomes too small, these particles could not provide a termination mechanism for the craze. In addition, these small dispersed particles would make an excessive stress concentration in PLA matrix.

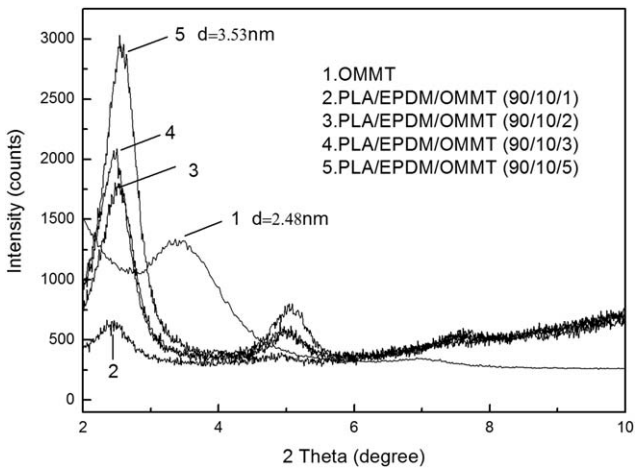

Figure 7. XRD patterns of pristine OMMT and PLA/EPDM/OMMT (90/10/x) samples.

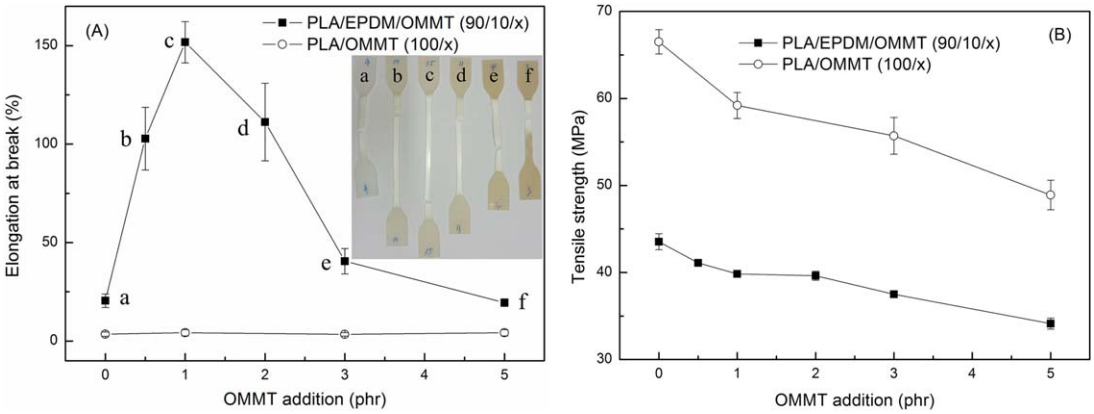

Figure 8. Elongation at break (A) and the inserted picture of tensile-fractured samples; tensile strength (B) *vs.* OMMT loading plots of PLA/EPDM/OMMT (90/10/x) and PLA/OMMT (100/x) samples. [Color figure can be viewed in the online issue, which is available at wileyonlinelibrary.com.]

Large crazes are therefore formed rapidly, causing early fracture. Moreover, an aggregation of OMMT particles is another adverse factor to weaken the ductility of PLA/EPDM/OMMT (90/10/x) samples when OMMT loading is more than 2 phr.

Similar results had been reported by Xiu *et al.* [23] The selective localization effect of SiO_2 nanoparticles on mechanical properties of PLA/PU/SiO_2 nanocomposites was investigated. It was found that SiO_2 nanoparticles selectively distributed at the interfacial surface of PU domains. And the incorporation of SiO_2 improved largely the tensile ductility of PLA/PU samples. It was confirmed that the optimum SiO_2 loading was 2.5 phr with a typical plastic deformation. If SiO_2 addition amounted up to 5 phr or higher, the elongation at break declined on the contrary due to the aggregation of SiO_2.

In addition, it is shown that the tensile strengths of PLA/EPDM/OMMT (90/10/x) and PLA/OMMT (100/x) samples decrease with increasing OMMT loading, which also results from the increase of stress concentration and the aggregation of OMMT particles.

Figure 9 shows relationship between OMMT loading and notched impact strength of PLA/EPDM/OMMT (90/10/x) samples. It indicates that the notched impact strength rises with certain amount of OMMT loading, however, then it falls which is consistent with the relationship between tensile ductility and OMMT loading. The notched impact strength enhances dramatically from 8.2 to 31.7 $kJ \cdot m^{-2}$ when OMMT loading increases from 0 to 1 phr. However, the impact toughness decreases sharply to 13.8 $kJ \cdot m^{-2}$ with further increasing OMMT loading to 5 phr. The impact resistance reaches to the best point with 1 phr OMMT, which is nearly 4 times over that of PLA/EPDM (90/10) blend and more than 6 times over that of neat PLA (4.8 $kJ \cdot m^{-2}$). Furthermore, to investigate the effect of OMMT on the toughness of PLA matrix, the notched impact strengths of PLA/OMMT (100/x) with various OMMT loadings aslo were presented in Figure 9. It can be seen that OMMT only has a slight toughening effect on PLA matrix without the presence of EPDM phase.

Figure 10 shows the notched impact fractured surface of PLA/EPDM/OMMT (90/10/x) samples with various OMMT loadings. It is found that the notched impact fractured surface of PLA/EPDM (90/10) sample is semi-brittle with little plastic deformation of PLA matrix, as shown in Figure 10(A). In contrast, the notched impact fractured surfaces of PLA/EPDM/OMMT (90/10/1) and PLA/EPDM/OMMT (90/10/2) show more plastic deformation of the matrix, as shown in Figure 10(B,C), respectively. The enhancement in impact toughness can also be explained by the crazing with shear yielding mechanism. The refinement in EPDM domain size and the increase in EPDM particle number show a significant effect to prevent the emergence and development of crack, allowing significant plastic deformation of PLA matrix to generate, leading to large energy consumption and eventually acquire higher impact toughness. Previously, similar conclusions were given in the researches of PLA/PU/TiO_2 and epoxy/acrylic/OMMT systems by Xiu and Balakrishnan, respectively.[15,24] The nanoparticles distribution at the interface in these blends was advantageous to the matrix deformation to produce plastic deformation.

However, with further increasing the OMMT loading, the aggregation of nanoparticles is inevitable. In addition, when OMMT loading is more than 2 phr, the EPDM particles become less

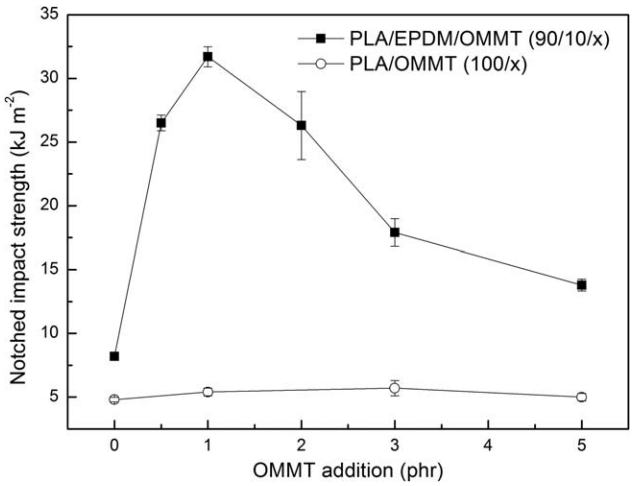

Figure 9. Plots of notched impact strength vs. OMMT loading of PLA/EPDM/OMMT (90/10/x) and PLA/OMMT (100/x) samples.

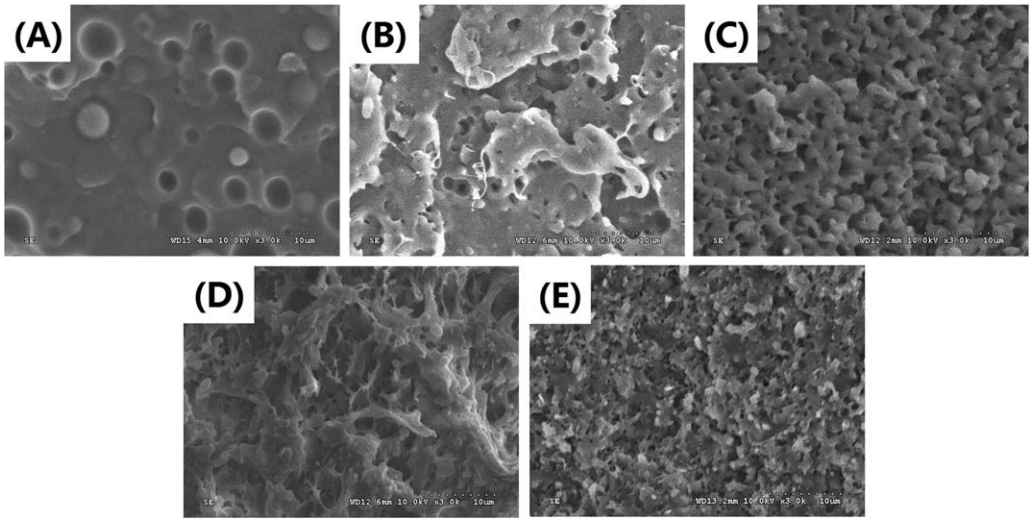

Figure 10. SEM micrographs of notched impact fractured surfaces of PLA/EPDM/OMMT (90/10/x) samples: (A) PLA/EPDM (90/10); (B) PLA/EPDM/OMMT (90/10/1); (C) PLA/EPDM/OMMT (90/10/2); (D) PLA/EPDM/OMMT (90/10/3); (E) PLA/EPDM/OMMT (90/10/5).

than 1μm that would make an excessive stress concentration in PLA matrix. Due to the OMMT aggregation and excessive stress concentration, large crazes are therefore formed rapidly, causing early fracture of the specimens under striking.

Blown Film of PLA/EPDM/OMMT (90/10/x) Nanocomposites

Attempts were made to produce ductile films from the PLA/EPDM/OMMT (90/10/x) nanocomposites by using blown film extrusion. Effects of OMMT on blown film bubble stability and tensile property of PLA/EPDM films were investigated. Figure 11 presents the comparison of the bubble shape of PLA, PLA/EPDM (90/10), PLA/EPDM/OMMT (90/10/1), and PLA/OMMT/OMMT (90/10/2) samples. As shown in Figure 11(A), the bubble of neat PLA film is transparent. However, with the addition of EPDM, the bubble of PLA/EPDM (90/10) film became translucent. The opacity is caused by the presence of EPDM phase with different refractive indices.[25]

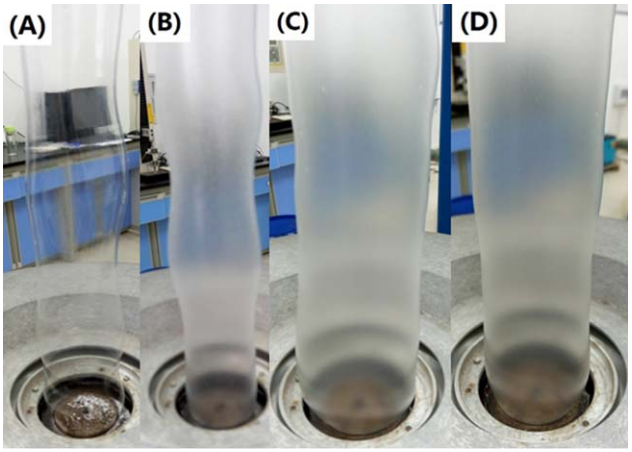

Figure 11. Comparison of bubble shapes of (A) neat PLA, (B) PLA/EPDM (90/10), (C) PLA/EPDM/OMMT (90/10/1), (D) PLA/EPDM/OMMT (90/10/2). [Color figure can be viewed in the online issue, which is available at wileyonlinelibrary.com.]

Figure 11(A) shows an unstable behavior of PLA encountered in blown film extrusion process. The limited blowing ability of PLA can be attributed to weak melt strength of PLA. [1] However, when 10% of EPDM was incorporated into PLA matrix, PLA/EPDM melt showed no obvious improvement in the blown film bubble stability, as shown in Figure 11(B). Figure 11(C,D) presents the bubble shape of PLA/EPDM/OMMT (90/10/1) and (90/10/2), respectively, during blown film extrusion. Notably, the incorporation of a small amount of OMMT into PLA/EPDM (90/10) can lead to a significant enhancement in the blown film bubble stability.

It can be attributed to the enhancement of melt strength resulted from the incorporation of OMMT. Because OMMT nanoparticles possess very large specific surface area and lot of active spots, a large number of PLA and EPDM molecules can be absorbed onto the surface of OMMT. The attractive interaction between OMMT surfaces and polymer chains would increase the melt strength and result in higher melt viscosity.[11,26] Consequently, stable bubbles of PLA/EPDM/OMMT nanocomposites during blown film extrusion were achieved.

Table II shows the tensile property of blown films of the PLA/EPDM (90/10) blends with and without OMMT. As expected, both the tensile performances in machine direction (MD) and

Table II. Tensile Properties of the Blown Films of PLA/EPDM Blends with and without OMMT

	Tensile strength (MPa)		Elongation at break (%)	
Film sample	MD	TD	MD	TD
PLA/EPDM (90/10)	24.2	19.6	24.4	5.3
PLA/EPDM/OMMT (90/10/1)	34.0	25.8	193.4	68.7
PLA/EPDM/OMMT (90/10/2)	33.4	28.7	213	67.1

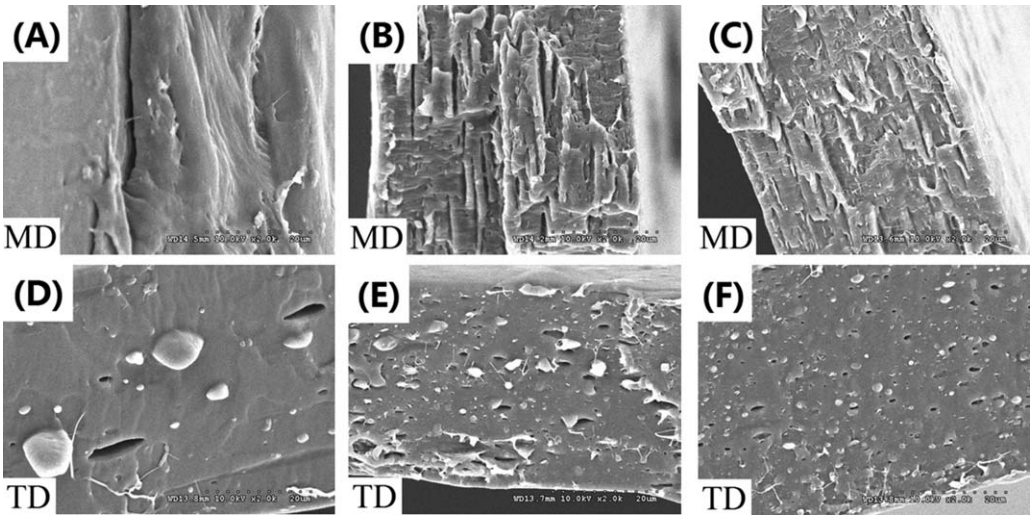

Figure 12. SEM micrographs of PLA/EPDM/OMMT (90/10/x) films in different directions (MD and TD): (A, D) PLA/EPDM (90/10); (B, E) PLA/EPDM/OMMT (90/10/1); (C, F) PLA/EPDM/OMMT (90/10/2).

transverse direction (TD) show a significant increase when OMMT was incorporated into PLA/EPDM (90/10) blend, compared with those of PLA/EPDM (90/10) film without OMMT. The enhancement in tensile ductility of PLA/EPDM/OMMT films can be attributed to the fact that the compatibilizing effect of OMMT. It must be pointed out that the tensile strength and elongation at break in TD are obviously less than those in MD for each film sample, which can be resulted from a lower BUR (ranged from 1.5 to 2.0) than TUR (around 5.5). Similar results were also given by other researchers.[27] Considering that the film stretching in TD and MD directions would cause microstructure orientation, and lead to a difference in tensile ductility of the films in TD and MD, micromorphologies of films' sections in MD and TD were observed, as shown in Figure 12. It is found that the dispersed EPDM phase presents itself as an elongated and fibrillar structure, preferably arranged toward the taken-up direction (i.e., MD). Because the TUR is obviously larger than the BUR, the initial spherical EPDM particles would be elongated toward MD during film extrusion, and finally formed a fibrillar structure in the obtained films. When the films were cold drawn along MD with the introduction of tensile load, the fibrillar EPDM phases aligned along MD could enhance the shear fracture resistance ability, and increase the craze termination probability. However, it is confirmed from Figure 12 that the cross-sectioned shape of EPDM phase along TD is almost circular due to the relatively low BUR of the films. Compared with the fibrillar structure aligned along MD, the circular section shape of EPDM phase along TD would show decreased shear fracture resistance ability and the craze termination ability when the films are stretched under a tensile load along TD.

Moreover, the incorporation of OMMT shows an obvious thinning effect on the fibrillar EPDM phase, as shown in Figure 12. The refinement of fibrillar EPDM phase certainly leads to an increase in the number of EPDM phase, which is helpful to terminate the craze and improve the tensile ductility of films.

CONCLUSIONS

PLA/EPDM/OMMT (90/10/x) nanocomposites with various OMMT loadings were prepared by a counter-rotating twin screw extruder. SEM micrographs showed a size reduction of the dispersed phases with the incorporation of OMMT, indicating a remarkable compatibilizing effect of OMMT in the immiscible PLA/EPDM blend. According to TEM observation, a large number of OMMT nanoparticles concentrated at the interfacial region between PLA and EPDM phases, as well as in EPDM phase due to higher affinity of OMMT with EPDM. The size reduction in EPDM domains was believed to be the main reason for the largely enhanced toughness of PLA/EPDM blend according to the crazing with shear yielding mechanism. When 1phr OMMT was incorporated into PLA/EPDM blend, the elongation at break and notched impact strength of PLA/EPDM/OMMT sample reached to the maximum values. Furthermore, OMMT significantly improved the blown film bubble stability and tensile ductility of PLA/EPDM/OMMT films. It can be concluded that OMMT is an efficient compatibilizer, as well as a processing aids for PLA/EPDM blends.

ACKNOWLEDGMENTS

The authors gratefully acknowledge support from Analytical and Testing Center of Hainan University. The authors also thank the support from National Science Foundation of China (grant number: 51263007), Enterprises-Universities-Researches Integration Project of Hainan Province of China (grant number: cxy20150023), and Natural Science Foundation of Hainan Province of China (grant number: 514206)

REFERENCES

1. Lim, L. T.; Auras, R.; Rubino, M. *Prog. Polym. Sci.* **2008**, *33*, 820.

2. Liu, H.; Zhang, J. *J. Polym. Sci. Part B: Polym. Phys.* **2011**, *49*, 1051.
3. Imre, B.; Bedő, D.; Domján, A.; Schön, P.; Julius Vancso, G.; Pukánszky, B. *Eur. Polym. J.* **2013**, *49*, 3104.
4. Feng, F.; Ye, L. *J. Macromol. Sci. Part B: Phys* **2010**, *49*, 1117.
5. As'habi, L.; Jafari, S. H.; Khonakdar, H. A.; Boldt, R.; Wagenknecht, U.; Heinrich, G. *Express Polym. Lett.* **2012**, *7*, 21.
6. Han, J. J.; Huang, H. X. *J. Appl. Polym. Sci* **2011**, *120*, 3217.
7. Zhao, F.; Huang, H. X.; Zhang, S. D. *J. Appl. Polym. Sci* **2015**, *132*, DOI: 10.1002/app.42511.
8. Al-Itry, R.; Lamnawar, K.; Maazouz, A. *Rheol. Acta* **2014**, *53*, 501.
9. Wang, Y.; Fu, Q.; Li, Q.; Zhang, G.; Shen, K.; Wang, Y. Z. *J. Polym. Sci. Part B: Polym. Phys.* **2002**, *40*, 2086.
10. Wang, X. H.; Zhang, H. X.; Jiang, W.; Wang, Z. G.; Liu, C. H.; Liang, H. J.; Jiang, B. Z. *Polymer* **1998**, *39*, 2697.
11. Zhang, Q.; Yang, H.; Fu, Q. *Polymer* **2004**, *45*, 1913.
12. Yang, H.; Zhang, X.; Qu, C.; Li, B.; Zhang, L.; Zhang, Q.; Fu, Q. *Polymer* **2007**, *48*, 860.
13. Gelfer, M. Y.; Song, H. H.; Liu, L.; Hsiao, B. S.; Chu, B.; Rafailovich, M.; Si, M.; Zaitsev, V. *J. Polym. Sci. Part B: Polym. Phys.* **2003**, *41*, 44.
14. Shi, Y.; Li, Y.; Xiang, F.; Huang, T.; Chen, C.; Peng, Y.; Wang, Y. *Polym. Adv. Technol.* **2012**, *23*, 783.
15. Xiu, H.; Bai, H. W.; Huang, C. M.; Xu, C. L.; Li, X. Y.; Fu, Q. *Express Polym. Lett.* **2013**, *7*, 261.
16. Yu, F.; Huang, H. X. *Polym. Test.* **2015**, *45*, 107.
17. Arruda, L. C.; Magaton, M.; Bretas, R. E. S.; Ueki, M. M. *Polym. Test.* **2015**, *43*, 27.
18. Chinsirikul, W.; Rojsatean, J.; Hararak, B.; Kerddonfag, N.; Aontee, A.; Jaieau, K.; Kumsang, P.; Sripethdee, C. *Packag. Technol. Sci.* **2015**, *28*, 741.
19. Liu, L.; Wang, Y.; Li, Y.; Wu, J.; Zhou, Z.; Jiang, C. *Polymer* **2009**, *50*, 3072.
20. Xiang, F.; Wu, J.; Liu, L.; Huang, T.; Wang, Y.; Chen, C.; Peng, Y.; Jiang, C.; Zhou, Z. *Polym. Adv. Technol.* **2011**, *22*, 2533.
21. Wang, B.; Wan, T.; Zeng, W. *J. Appl. Polym. Sci.* **2012**, *125*.
22. Bucknall, C. B.; Reddock, S. E.; Keast, W. E. *J. Mater. Sci.* **1984**, *7*, 808.
23. Xiu, H.; Huang, C.; Bai, H.; Jiang, J.; Chen, F.; Deng, H.; Wang, K.; Zhang, Q.; Fu, Q. *Polymer* **2014**, *55*, 1593.
24. Balakrishnan, S.; Start, P. R.; Raghavan, D.; Hudson, S. D. *Polymer* **2005**, *46*, 11255.
25. Zhang, W.; Gui, Z.; Lu, C.; Cheng, S.; Cai, D.; Gao, Y. *Mater. Lett.* **2013**, *92*, 68.
26. Si, M.; Araki, T.; Ade, H.; Kilcoyne, A. L. D.; Fisher, R.; Sokolov, J. C.; Rafailovich, M. H. *Macromolecules* **2006**, *39*, 4793.
27. Sodergard, A.; Selin, J. F.; Niemi, M.; Nasman, J. H. Processable Poly(hydroxy acids): US, US6559244[P]. **2003**.